ELSEVIER

Physica B 241–243 (1998) 511–516

PHYSICA B

Neutron scattering studies of geometrically frustrated pyrochlore antiferromagnets

B.D. Gaulin[a,*], J.S. Gardner[a], S.R. Dunsiger[b], Z. Tun[c], M.D. Lumsden[a], R.F. Kiefl[b], N.P. Raju[d], J.N. Reimers[e], J.E. Greedan[d]

[a] *Department of Physics and Astronomy, McMaster University, Hamilton, ON, Canada,* L8S 4M1
[b] *Department of Physics and Astronomy, University of British Columbia, Vancouver, BC, Canada,* V6T 1Z1
[c] *National Research Council, Neutron Program for Materials Research, Chalk River Laboratories, Chalk River, ON, Canada,* K0J 1J0
[d] *Department of Chemistry, McMaster University, Hamilton, ON, Canada,* L8S 4M1
[e] *Moli Energy (1990) Ltd., Maple Ridge, BC, Canada,* V2X 9E7

Abstract

Elastic and inelastic neutron scattering work on the cubic pyrochlore antiferromagnets $Y_2Mo_2O_7$, $Tb_2Ti_2O_7$, and $Tb_2Mo_2O_7$ is reviewed. These materials are characterized by antiferromagnetically coupled moments residing on a network of corner-sharing tetrahedra. Geometrical frustration manifests itself strongly in such systems in that two of them display a spin-glass-like transition in the apparent absence of chemical disorder, while the other remains paramagnetic to at least 0.1 K, despite developing antiferromagnetic short-range order at 50 K.

Keywords: Geometrical frustration; Antiferromagnetism; Spin-glass-like state

The combination of near-neighbour antiferromagnetic interactions and certain lattice symmetries, based on triangles and tetrahedra, lead to phenomena known as geometrical frustration [1]. A triad of near-neighbour spins with triangular coordination cannot each be mutually antiparallel to its neighbours, and consequently a simple two-sublattice Néel state is not possible at low temperatures. The tetrahedron is the three-dimensional analogue of the triangle in this regard, and such combinations are common in nature. Real crystals may be comprised of magnetic atoms residing on lattices made of edge- or corner-sharing triangles as well as edge- and corner-sharing tetrahedra.

Many cubic pyrochlores are of the chemical formula $A_2B_2O_7$, where the A site is occupied by a tri-valent rare-earth ion, with eightfold oxygen coordination, and the B site is occupied by a tetravalent transition-metal ion, with sixfold oxygen coordination [2]. Both the A and B sites individually form a network of corner-sharing tetrahedra, as shown in Fig. 1, and if either site is magnetic with antiferromagnetic near-neighbour interactions, then a high degree of frustration must be present.

*Corresponding author. Tel.: 905 525 9140 x24362; fax: 905 546 1252; e-mail: gaulin@mcmaster.ca.

0921-4526/98/$19.00
PII S0921-4526(97)00631-5

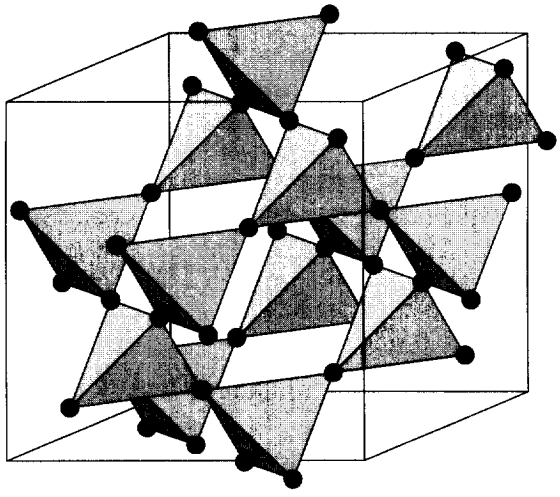

Fig. 1. The network of corner-sharing tetrahedra which, individually, both the A and B atom sublattices of the $A_2B_2O_7$ cubic pyrochlores display. Unit cell dimensions are very similar in all three pyrochlores discussed, ~ 10 Å.

In this paper, we review our recent neutron-scattering studies of three such pyrochlore antiferromagnets: $Tb_2Ti_2O_7$, $Y_2Mo_2O_7$, and $Tb_2Mo_2O_7$. The first two of these are examples where only the A or B sites are magnetic, while the third contains magnetic species at both the A and B sites.

Theoretical arguments have been made which lead to large ground-state degeneracies for both Ising [3–7] and continuous [4–8] (XY and Heisenberg) spins residing on the pyrochlore lattice. For near-neighbour antiferromagnetic interactions, local ordering of the spins on a single tetrahedron subject to the constraint $\sum_i \boldsymbol{S}_i = 0$, where the sum is over those spins on a single tetrahedron, is expected with no long-range order. Villain [8] coined the term "co-operative paramagnetism" to describe such a state at low temperature. There is at least one known example of an antiferromagnetic pyrochlore in which a coherent ordered state consistent with the $\sum_i \boldsymbol{S}_i = 0$ constraint forms at low temperature. This is FeF_3 [9] which enters a non-collinear, four-sublattice antiferromagnetic state below ~ 18 K.

The uniform susceptibilities exhibited by both $Tb_2Ti_2O_7$ and $Y_2Mo_2O_7$ are well described by a Curie–Weiss form at high temperatures, with $\theta_{CW} \sim -19$ and -201 K, respectively, indicating antiferromagnetic near-neighbour interactions between the Tb^{3+} or Mo^{4+} moments. The paramagnetic moment at each site is 9.4 and $2.55\mu_B$, respectively, roughly consistent with the free-ion value for Tb^{3+}, and a spin-1 moment for Mo^{4+}. A similar analysis in $Tb_2Mo_2O_7$ is more complicated due to the presence of two interacting moments. At low temperatures, the susceptibilities are strikingly different in the two single-magnetic site pyrochlores, with $Tb_2Ti_2O_7$ displaying paramagnetic behaviour to the lowest temperatures measured, while $Y_2Mo_2O_7$ displays classic spin-glass behaviour near $T_g \sim 22$ K, including both history dependences and a divergence of its non-linear susceptibility [10]. This behaviour is shown in Fig. 2.

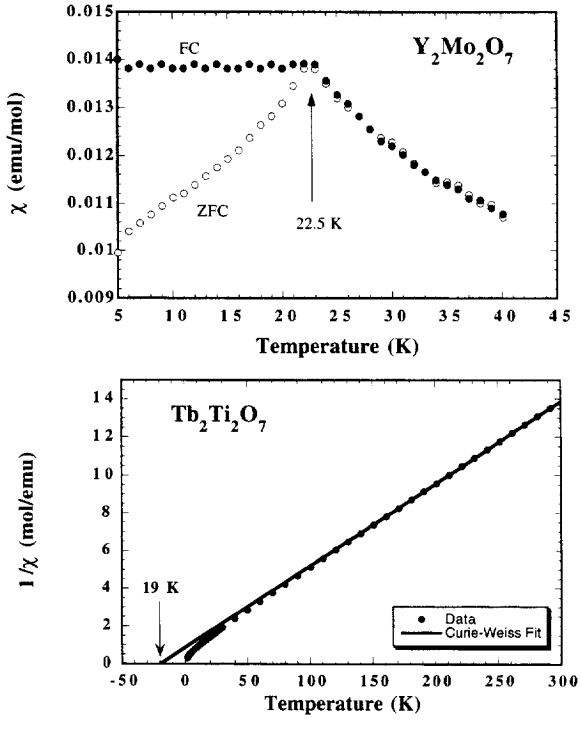

Fig. 2. top: The low-temperature susceptibility exhibited by $Y_2Mo_2O_7$ is shown. A clear break between the field-cooled (FC) and zero-field-cooled (ZFC) susceptibilities indicates the appearance of the spin-glass state(below $T_g \sim 22.5$ K. bottom: The inverse of the uniform susceptibility, measured in a 0.01 T magnetic field, is shown as a function temperature for $Tb_2Ti_2O_7$, along with a fit of the high-temperature regime of this data to a Curie–Weiss form.

$Tb_2Mo_2O_7$ also displays spin-glass anomalies at $T_g \sim 25$ K, and the similarity of this value of T_g to that displayed by $Y_2Mo_2O_7$ is strongly suggestive that the spin-glass phenomena is driven by the Mo^{4+} sublattice. That this occurs in nominally pure magnetic materials (non-stoichiometric oxygen content is the most likely form of chemical disorder. However, diffraction profile refinement indicate that any such non-stoichiometry must be below the 1% level [2,11].) is a substantial challenge to theory.

The top panel of Fig. 3 shows the results of neutron powder diffraction studies on both $Tb_2Ti_2O_7$ at 2.5 K and $Tb_2Mo_2O_7$ at 12 K, taken at the NRU reactor of the Chalk River Laboratories (CRL) with neutrons of frequency $E/h = 3.52$ THz, and a pyrolitic graphite filter in the beam to remove higher-order contamination. Sharp, resolution-limited nuclear Bragg peaks can be seen

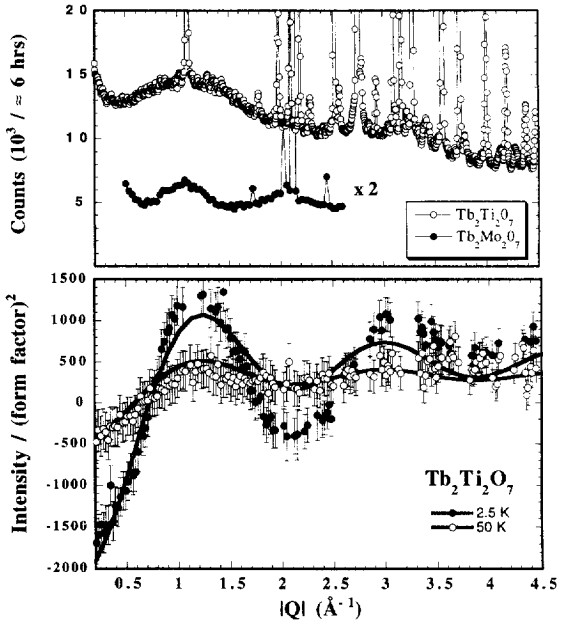

Fig. 3. Top panel: Neutron powder diffraction patterns using 3.52 THz neutrons from $Tb_2Ti_2O_7$ at 2.5 K and $Tb_2Mo_2O_7$ at 12 K is shown. Bottom panel: The difference between diffraction patterns of $Tb_2Ti_2O_7$ taken at (i) 2.5 K and (ii) 50 K and that taken at 100 K, corrected for the Tb^{3+} magnetic form factor, is shown. The solid lines are fits of the net intensity data set to the scattering expected from spins correlated over a single tetrahedron only, and taking up the local structure displayed by FeF_3.

superposed on a diffuse distribution of magnetic scattering in the case of $Tb_2Ti_2O_7$. A similar distribution of magnetic scattering is also observed in $Tb_2Mo_2O_7$, although the periodicity of the diffuse magnetic scattering is clearly different, and the nuclear peaks over this range of $|\boldsymbol{Q}|$-space are relatively weaker. The bottom panel of Fig. 3 shows neutron diffraction data sets from $Tb_2Ti_2O_7$ at 2.5 and 50 K, in which a high-temperature data set at 100 K has been subtracted and the net intensity has been corrected for the $|\boldsymbol{Q}|$-dependence of the Tb^{3+} magnetic form factor. This net intensity can then be easily compared to a calculation of the scattering expected from spin correlations extending over a single tetrahedron only. We have chosen to calculate the scattering expected from the local, four sublattice, antiferromagnetic structure displayed by FeF_3 [9]. This local structure is not, of course, unique, but it is consistent with the $\sum_i \boldsymbol{S}_i = 0$ constraint, and has the moments at the eightfold-coordinated Tb^{3+} site aligned along the eight [1, 1, 1] cubic symmetry directions. As will be discussed, inelastic neutron scattering provides clear evidence for substantial single-ion anisotropy in the Tb^{3+} moments. The form of the scattering from a polycrystal displaying such a local structure is [12]

$$I(Q) \sim \sum_{i,j} \langle S_i \cdot S_j \rangle \frac{\sin(Qr_{i,j})}{Qr_{i,j}}, \tag{1}$$

which simplifies to

$$I(Q) \sim \frac{\sin(Qr_{i,j})}{Qr_{i,j}} \tag{2}$$

if spins are coordinated over near-neighbours, and consequently one value of $r_{i,j}$ (the distance between spins at sites i and j), only. The fit of the model to the net intensity at 2.5 and 50 K is shown as the solid lines in the bottom panel of Fig. 2. As can be seen, this simple model provides a good description of the measured net intensity, correctly accounting for the positions of the peaks and valleys. Interestingly, the inclusion of spin correlations beyond nearest neighbours produces peaks in the calculated net intensity intermediate between those at ~ 1.2 Å^{-1} and ~ 3.1 Å^{-1}, as observed and perhaps expected in $Tb_2Mo_2O_7$, where spin-1 moments at the Mo^{4+} site can mediate longer-range

spin correlations. We therefore conclude that spins in $Tb_2Ti_2O_7$ are correlated over a single tetrahedron only down to at least 2.5 K, while those in $Tb_2Mo_2O_7$ are correlated over somewhat longer distances, at least to near-neighbour tetrahedra at low temperatures.

Inelastic neutron scattering measurements were carried out on the same sample of $Tb_2Ti_2O_7$, now mounted in a closed-cycle refrigerator with a base temperature of 12 K. Measurements were performed on the C5 triple-axis spectrometer at the CRL in constant scattered energy mode with $E'/h = 1.2$ THz and a cooled Be filter in the scattered beam. Typical constant $|\boldsymbol{Q}|$ scans are shown in the top panel of Fig. 4, taken at the base temperature. This panel shows constant $|\boldsymbol{Q}|$ scans at $|\boldsymbol{Q}| = 0.7, 1.2$, and $2.2\,\text{Å}^{-1}$. The energy of the modes at 0.7 and $2.2\,\text{Å}^{-1}$ are nearly identical, while there is a pronounced decrease in the integrated intensity of the mode at $2.2\,\text{Å}^{-1}$ compared with that at $0.7\,\text{Å}^{-1}$, consistent with that expected due to the Tb^{3+} magnetic form factor. The energy of these modes clearly dips near $1.2\,\text{Å}^{-1}$, and Gaussian fits to these and similar data at a variety of $|\boldsymbol{Q}|$'s bear this out, as is seen in the lower panel of Fig. 4. The energy of this mode dips by roughly 10%, at the wave vector corresponding to the first maximum in the magnetic structure factor (see Fig. 3).

At low temperatures where it is well developed, the incomplete softening of this well-defined branch of excitations bears a striking resemblance to the roton minimum which occurs in the single-particle excitation spectrum of liquid ^{4}He, wherein a 30% dip in the energy of the excitations occurs very near the first maximum of the liquid ^{4}He [13] structure factor. The minimum in the magnetic excitation spectrum in $Tb_2Ti_2O_7$ goes away with increasing temperature roughly as the structure in the elastic scattering goes away, and by 30 K it is no longer evident as seen in the bottom panel of Fig. 4, even though the excitations themselves are still well defined. On further increasing the temperature the mode weakens in intensity and has merged into the background by 100 K.

While a gapped magnetic excitation spectrum can arise in singlet ground state systems as occur in Haldane [14,15] and spin-Peierls [16] systems, such materials exhibit distinctive susceptibilities

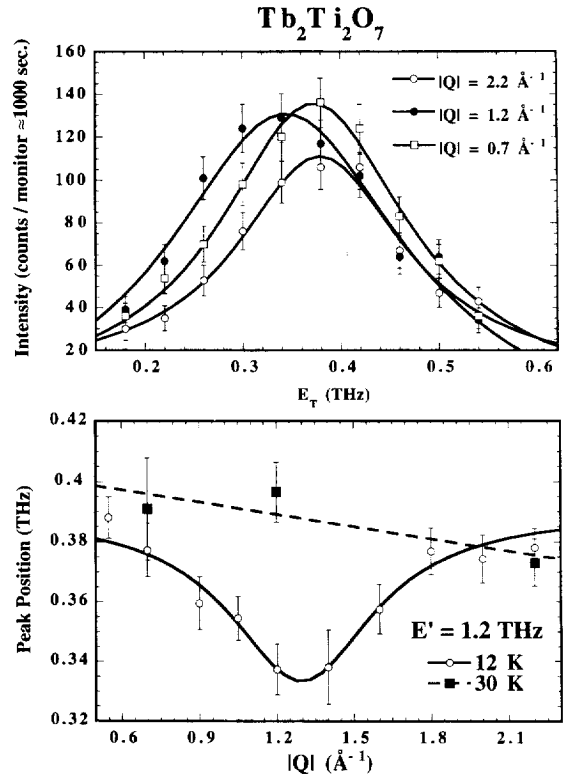

Fig. 4. Top panel: Constant $|\boldsymbol{Q}|$ scans of $Tb_2Ti_2O_7$ at 0.7, 1.2, and $2.2\,\text{Å}^{-1}$ at $T = 12$ K are shown. The neutron group at $1.2\,\text{Å}^{-1}$ is centred at a lower energy than those at 0.7 or $2.2\,\text{Å}^{-1}$. Bottom panel: The dispersion of the magnetic excitation spectrum at 12 and 30 K is shown. At 12 K a clear incomplete softening of the modes near the first maximum in the magnetic structure factor (see Fig. 3) is seen.

which tend rapidly to zero at low temperatures. Otherwise, such features are due to Ising-like anisotropy in the spin Hamiltonian, as would be expected due to orbital contributions to the Tb^{3+} magnetic moment in its crystalline environment with eightfold oxygen coordination. Employing our local FeF_3 [9] structure in which the moments align along the eight [1, 1, 1] directions, these measurements show that the anisotropy gap, the amount of energy that is required to displace the spins from this easy direction, is ~ 0.38 THz or 18 K. It is then possible to think of the dip in the excitation spectrum near $Q = 1.2\,\text{Å}^{-1}$, the "spin roton", as a collective tumbling of spin orientations on loosely correlated tetrahedra from one such

local ground state to another. The complete softening of this mode would precipitate a transition to a non-collinear ordered magnetic state as occurs in FeF_3 [1], but this does not occur in $Tb_2Ti_2O_7$, leaving it a co-operative paramagnet to low temperatures.

The temperature dependence of the magnetic diffuse scattering observed in $Tb_2Mo_2O_7$ [17,18] is quite similar to that seen in $Tb_2Ti_2O_7$. In both cases most of the liquid-like structure is gone by 100 K, and in the case of $Tb_2Mo_2O_7$, it is obvious to the spin-glass anomaly at $T_g \sim 25$ K. This reinforces the picture of the diffuse scattering arising from short-range order on the Tb^{3+} sublattice, and the spin-glass state being driven by the Mo^{4+} sublattice. Well-defined inelastic scattering, as seen in $Tb_2Ti_2O_7$, has not been observed in $Tb_2Mo_2O_7$. This may be due to more pronounced dispersion in the excitation spectrum due to interactions between the Tb^{3+} and Mo^{4+} sublattices. A powder average of an excitation spectrum with substantial dispersion would wash out any well-defined inelastic features. The frequency width of the quasi-elastic scattering from $Tb_2Mo_2O_7$ does exhibit narrowing on entering the spin-glass phase [18]. This frequency width is close to the resolution limit for measurements with scattered neutrons of frequency $E/h = 1.1$ THz, but these measurements are nicely consistent with μSR determinations of the spin relaxation which can be made to much lower frequencies than are accessible to neutrons [19].

The scattering from polycrystalline $Y_2Mo_2O_7$ proved to be more difficult to study. Very recent results [20] show diffuse magnetic scattering peaking up near $|Q| \sim 0.45$ Å^{-1}, indicative of local spin configurations more complicated than those displayed by $Tb_2Ti_2O_7$. Inelastic scattering at small $|Q|$, and therefore identified as magnetic in origin, has been observed and is shown in Fig. 5. This scattering, taken on the C5 triple-axis spectrometer at CRL was obtained with neutrons of fixed-scattered frequency $E/h = 6$ THz, and Fig. 5 shows a constant $|Q| = 0.8$ Å^{-1} scan taken at 10 K (less than half of T_g), 30 K (just above T_g) and 230 K ($\sim 10 \times T_g$ and roughly θ_{CW}). A flat background has been subtracted and a clear temperature-dependent inelastic signal is seen. On the neutron-energy loss side (+ve side) the distribution of

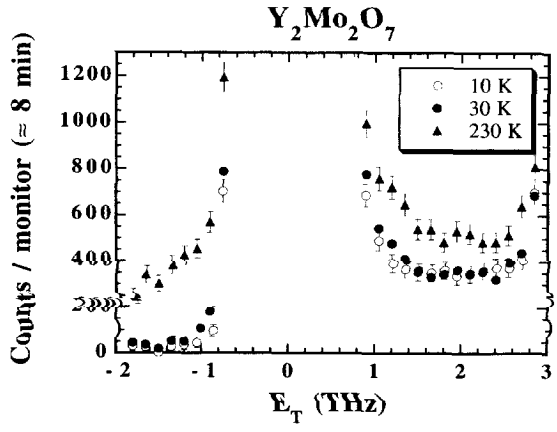

Fig. 5. Constant $|Q|$ scans of $Y_2Mo_2O_7$ powder at 0.8 Å^{-1} and temperatures of 10, 30 and 230 K are shown. A constant background has been subtracted.

inelastic scattering is remarkably flat out up to 3 THz, where the incident beam begins to interfere with the measurement. The absence of scattering on the energy-gain side of zero-energy transfer indicates that this signal is real (as opposed to background) as it satisfies detailed balance. These data show the inelastic spectrum to be extended in frequency with no obvious decrease in density of states beyond $E/h \sim 3$ THz. Kinematic considerations limit the range of frequencies which can be investigated at these low wave vectors, but we may expect the cutoff for the extent of this spectrum to be set by at least $|\theta_{CW}| \sim 200$ K ~ 4 THz. This inelastic spectrum is more extended in frequency than occurs in either the well-studied pyrochlore-slab (or Kagomé-like) compound $SrCr_{(8-x)}Ga_{4+x}O_{19}$ [21] or the disordered pyrochlore system $CsNiCrF_6$ [22]. As is the case in both of these systems, the present results suggest a strongly fluctuating nature to the spin-glass state in $Y_2Mo_2O_7$ at low temperatures [23].

As expected, the spin-glass features at $T_g \sim 22$ K are not manifest in any of these high-frequency inelastic scattering results, as $T_g \sim 0.5$ THz. Such effects have been seen in very recent low-frequency inelastic scattering results [20], as well as in the spin relaxation rate [19] obtained from μSR at frequencies substantially lower than can be probed with neutrons.

To conclude, our studies of $Y_2Mo_2O_7$ and $Tb_2Ti_2O_7$ reveal strong but different manifestations of geometrical frustration in their antiferromagnetic behaviour. While significant progress has been made, important questions remain open as to what microscopic features in the Hamiltonians of these two systems are responsible for their differing ground states. Measurements extended to single crystal samples are expected to be important in elucidating such questions.

References

[1] For recent reviews see: A.P. Ramirez, Ann. Rev. Mater. Sci. 24 (1994) 453. H.T. Diep (Ed.), Magnetic Systems with Competing Interactions, World Scientific, Singapore, 1994; P. Schiffer, A.P. Ramirez, Commun. Condens. Matter Phys. 18 (1996) 21; B.D. Gaulin, M.J.P. Gingras, J. Phys.: Condens. Matter, to be published.
[2] M.A. Subramanian, G. Aravamudan, G.V. Subba Rao, Prog. Solid State Chem. 15 (1983) 55.
[3] P.W. Anderson, Phys. Rev. 102 (1956) 1008.
[4] J.N. Reimers et al., Phys. Rev. B 43 (1991) 865.
[5] J.N. Reimers, Phys. Rev. B 45 (1992) 7287.
[6] J.T. Chalker et al., Phys. Rev. Lett. 68 (1992) 855.
[7] J.N. Reimers, A.J. Berlinsky, Phys. Rev. B 48 (1993) 9539.
[8] J. Villain, Z. Phys. B 33 (1979) 31.
[9] G. Ferey, R. de Pape, M. Leblanc, J. Pannetier, Rev. Chim. Miner. 23 (1986) 474.
[10] M.J.P. Gingras, C.V. Stager, N.P. Raju, B.D. Gaulin, J.E. Greedan, Phys. Rev. Lett. 78 (1997) 947.
[11] J.N. Reimers, J.E. Greedan, R.K. Kremer, E. Gmelin, M.A. Subramanian, Phys. Rev. B 43 (1991) 3387.
[12] E.F. Bertaut, P. Burlet, Solid State Commun. 5 (1967) 279.
[13] H.R. Glyde, E.C. Svensson, Methods of Experimental Physics, vol. 23, ch. 13, Academic Press, San Diego, 1987, p. 303.
[14] R.M. Morra et al., Phys. Rev. B 38 (1988) 543.
[15] K. Kakurai et al., J. Phys.: Condens. Matter 3 (1991) 715.
[16] O. Fujita, J. Akimitsu, M. Nishi, K. Kakurai, Phys. Rev. Lett. 74 (1995) 16 and references contained therein.
[17] J.E. Greedan, J.N. Reimers, C.V. Stager, S.L. Penny, Phys. Rev. B 43 (1991) 5682.
[18] B.D. Gaulin, J.N. Reimers, T.E. Mason, J.E. Greedan, Z. Tun, Phys. Rev. Lett. 69 (1992) 3244.
[19] S.R. Dunsiger, R.F. Kiefl, K.H. Chow, B.D. Gaulin, M.J.P. Gingras, J.E. Greedan, A. Keren, K. Kojima, G.M. Luke, W.A. MacFarlane, N.P. Raju, J.E. Sonier, Y.J. Uemura, W.D. Wu, Phys. Rev. B 54 (1996) 9019.
[20] J.S. Gardner, S.H. Lee, C. Broholm, N.P. Raju, B.D. Gaulin, to be published.
[21] C. Broholm, G. Aeppli, G.P. Espinosa, A.S. Cooper, Phys. Rev. Lett. 65 (1990) 3173.
[22] M.J. Harris, M.P. Zinkin, Z. Tun, B.M. Wanklyn, I.P. Swainson, Phys. Rev. Lett. 73 (1994) 189.
[23] A.P. Ramirez et al., Phys. Rev. Lett. 64 (1990) 2070.